Photocatalysis Hot Paper

International Edition: DOI: 10.1002/anie.201511334
German Edition: DOI: 10.1002/ange.201511334

Oxide-Modified Nickel Photocatalysts for the Production of Hydrocarbons in Visible Light

Yufei Zhao[+], Bo Zhao[+], Jinjia Liu, Guangbo Chen, Rui Gao, Siyu Yao, Mengzhu Li, Qinghua Zhang, Lin Gu, Jinglin Xie, Xiaodong Wen, Li-Zhu Wu, Chen-Ho Tung, Ding Ma,* and Tierui Zhang**

Abstract: *Metallic nickel nanostructures that were partially decorated by discrete nickel oxide layers were fabricated by in situ reduction of calcinated Ni-containing layered double hydroxide nanosheets, the structure of which was confirmed by extended X-ray absorption fine structure spectroscopy, X-ray photoelectron spectroscopy, and transmission electron microscopy. The existence of the abundant interfaces between the surface Ni oxide overlayer and metallic Ni altered the geometric/electronic structure of the Ni nanoparticles, making them apt for CO activation under light irradiation. Most importantly, the unique structure favors the C–C coupling reaction on its surface, which confers the catalyst unexpected reaction power towards higher hydrocarbons at moderate reaction conditions. This study leads to a green and sustainable approach for the photocatalytic production of highly valuable chemical fuels.*

CO hydrogenation is an energy-alternative pathway to produce fuels and other chemicals. It happens on the surface of active metals through CO dissociation, hydrogenation, and chain propagation to produce long-chain hydrocarbon. The process is so-called Fischer–Tropsch synthesis (FTS).[1] The source of CO and H_2 (syngas) can be coal, natural gas (shale gas) as well as biomass, and residuum. FTS gains increasing economic interest due to the prominence of recently discovered large reserve of shale gas worldwide. Significantly, as coal is the main carbon resource (> 60%) in China, the green and sustainable transformation of coal through FTS to olefin and liquid fuels is of particular importance for a sustainable economic growth.

Among FTS catalysts, Ru, Co and Fe-based catalysts are extensively used in either fundamental researches or in industrial performance. Ni can also be a FTS catalyst, but it is more favorable for methane.[2] Although Ru, Co, Fe, and Ni are close neighbors in the periodic table, their catalytic performances and active phases in the FTS are different. The active phase of Ru, Co, and Ni-based catalysts is mainly the corresponding metal, while Fe-based catalyst can form a number of phases from metal to oxides to various carbides.[3] It is hard to determine their activity for the FTS since there are many factors influencing the catalytic performance, such as the reaction temperature, reaction pressure, and feedstocks.

A series of multi-step reactions with many parallel pathways are involved in the FTS. Among them, both to split a C–O bond and to form new C–C bonds are important steps. For instance, CO could go through the direct or hydrogen-assisted breakage over the active surface, leading to the formation of carbon-containing and oxygen-containing species on the surface. On the other hand, carbon-containing species could undergo C–C coupling and/or hydrogenation to produce higher hydrocarbons as well as methane.[2,4] Different from the reactions on Ru, Co, and Fe, the Ni catalyst favors the hydrogenation instead of the C–C coupling reaction at a high temperature (300–500 °C).[2] Consequently, the product is mainly methane, which is also known as the methanation reaction.[5] Occasionally, the formation of higher hydrocarbons could be observed on Ni-based catalysts, but in most cases, a second metal additive such as Fe/Co/Ru,[6] an alkali metal promoter[7] or an active oxide as support were required.[8]

Compared with thermal reactions, photocatalysis is one of the most sustainable and green solutions to address the current global energy and environmental issues by the efficient use of solar energy.[9] Recent investigations show that NiO and Ni-Al_2O_3 catalysts can catalyze the methanation of CO and CO_2 under visible or UV/Vis light irradiation,[10] with a selectivity toward methane of more than 97%. Subsequently, Ye and co-workers reported that nanoscaled group VIII metal-based catalysts showed an excellent performance for the hydrogenation of CO_2 to CH_4 at 573 K induced by the photothermal effect.[11]

[*] Dr. Y. Zhao,[+] G. Chen, Prof. L.-Z. Wu, Prof. C.-H. Tung, Prof. T. Zhang
Key Laboratory of Photochemical Conversion and Optoelectronic Materials
Technical Institute of Physics and Chemistry
Chinese Academy of Sciences
Beijing 100190 (China)
E-mail: tierui@mail.ipc.ac.cn

B. Zhao,[+] S. Yao, M. Li, J. Xie, Prof. D. Ma
College of Chemistry and Molecular Engineering
Peking University, Beijing 100871 (China)
E-mail: dma@pku.edu.cn

J. Liu, R. Gao, Prof. X. Wen
Institute of Coal Chemistry
Chinese Academy of Sciences & Synfuels China
Beijing (China)
E-mail: wxd@sxicc.ac.cn

Dr. Q. Zhang, Prof. L. Gu
Beijing National Laboratory for Condensed Matter Physics
Institute of Physics, Chinese Academy of Sciences
Beijing, 100190, China

[+] These authors contributed equally to this work.

Supporting information for this article can be found under http://dx.doi.org/10.1002/anie.201511334.

An interesting question arises: could one make Ni be more efficient for the C–C coupling reaction instead of the methanation under visible-light irradiation, especially at a low reaction temperature? Here we demonstrate that by using NiO_x supported Ni (NiO_x/Ni) obtained by reducing calcinated Ni-containing layered double hydroxides (LDHs) as the photocatalyst, an extraordinarily high selectivity for the C_{2+} hydrocarbons (maximum 80%) can be achieved for the hydrogenation of CO. The key for the unique catalytic performance was the existence of discrete NiO_x overlayers on the surface of metallic Ni nanoparticles. Besides the capability of absorbing UV and/or visible light, the high activity of hydrogenation on a metallic Ni surface has been restrained by the modulation of interfacial NiO_x, and the C–C coupling was favored at the same time. As a result, the novel Ni catalytic system with photocatalytic activity for syngas conversion to higher hydrocarbons was constructed. This work highlights the possibility of using solar energy to produce fuel/chemicals by using Ni-based catalyst under mild reaction conditions.

The NiO_x/Ni catalysts were prepared by reducing the calcinated Ni-containing LDH precursor (samples before and after calcination are denoted as NiAl-LDH and NiAl-MMO, respectively) from 100 to 600 °C (denoted as Ni-*x*, *x* means the reduction temperature). Before calcination, the NiAl-LDH sample showed typical (00*l*) basal reflections which are characteristic of layered structures.[12] After calcination, the basal reflections disappeared while new signals appeared, suggesting the generation of NiO and amorphous Al_2O_3 (see Figure S1 in the Supporting Information). In situ X-ray diffraction (XRD) patterns of NiAl-MMO during the reduction process indicate that, at a reduction temperature of 100–450 °C (Figure 1 A), the dominant phase was NiO while a new phase corresponding to metallic Ni appeared when the reduction temperature reached 500 °C, which is consistent with the temperature-programmed reduction (TPR) result (Figure S2). The intensity of metallic Ni signal increased with increasing reduction temperature (from 500 to 600 °C) and became the dominant phase at 600 °C.

Since the UV/Vis absorption behavior is associated with the photoinduced electron-transfer process of photocatalysts, the diffuse reflectance UV/Vis spectra of Ni-*x* were measured (Figure 1 B). Compared with the intense absorption mostly at the UV range for NiAl-MMO, the whole range absorption capability was observed for Ni-*x*, which is consistent with the color change of the samples (Figure S3). These catalysts as well as the reference catalysts were used in photocatalytic CO hydrogenation reactions under UV/Vis light irradiation (0.8 bar, H_2/CO = 1/3, room temperature). The results are summarized in Table 1. Under irradiation, NiO, NiAl-MMO and commercial Ni/Al_2O_3 are almost inactive for CO activation, with a CO conversion of less than 5%. Most of the converted CO has been transformed into CO_2 with a selectivity of over 74%. When Ni-500 was used as the catalyst, a low catalytic activity was observed (Table 1, entry 6). However, the reaction channel towards CO_2 was suppressed (selectivity of 6.2%). Surprisingly, besides methane, a large amount of higher hydrocarbons were produced (Table 1 and Figure S4). When the reduction temperature reached 525 °C, the conversion of CO increased sharply to 27.7%, with a rather higher selectivity for hydrocarbons (60.1%). The selectivity for hydrocarbon products follows the Anderson-Schulz–Flory (ASF) distribution (Figure S5), with a relatively small growth factor (α) of 0.60. The carbon source of the hydrocarbons was CO as confirmed by control experiment using pure hydrogen (Table 1, entry 2) and isotopically labeling experiments using ^{13}CO as feeds over Ni-525 (Figure S6). This indicates that, different from conventional Ni-based catalysts where the dominant product of CO hydro-

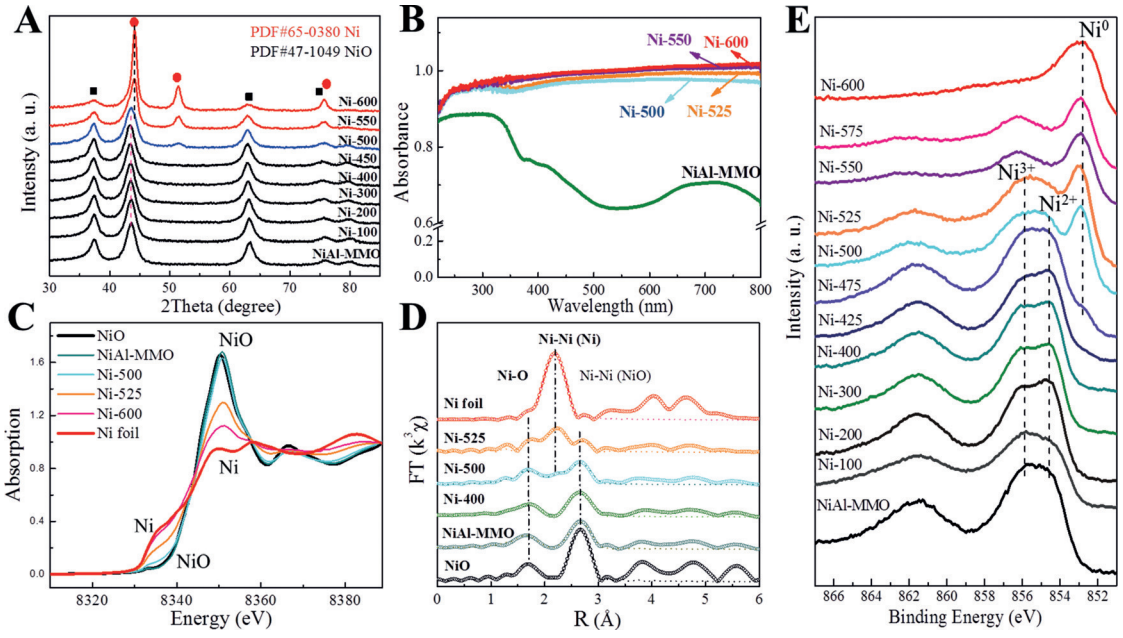

Figure 1. A) In situ XRD patterns of NiAl-MMO and Ni-*x*. B) UV/Vis spectra of Ni-*x*. C) Ni K-edge XANES and D) EXAFS of NiAl-MMO and Ni-*x*. E) In situ XPS spectra of NiAl-MMO and the samples reduced at different temperatures (Ni-*x*).

Table 1: Photocatalytic performance of Ni-based catalysts.[a]

Entry	Photocatalyst	CO Conversion [%]	Selectivity [%]			
			C_2–C_4	C_5–C_7	CH_4	CO_2
1	blank[b]	0	–	–	–	–
2	Ni-525[c]	–	–	–	–	–
3	Ni-Al_2O_3[d]	4.7	6.9	2.7	10.8	79.6
4	NiAl-MMO	2.1	2.5	1.4	19.8	76.3
5	NiO	1.5	1.5	0.8	23.3	74.4
6	Ni-500	2.6	38.2	16.2	39.4	6.2
7	Ni-525	27.7	37.4	21.1	38.8	2.7
8	Ni-550	56.4	27.3	10.2	62.4	0.1
9	Ni-600	95.8	19.9	5.6	73.4	1.1
10	Ni-525[e]	20.9	44.3	22.8	30.9	2.0
11	Ni-525[f]	33.7	33.4	13.5	44.3	8.8

[a] Reaction conditions: no external heating, 0.08 MPa, $CO/H_2/Ar = 20/60/20$, catalyst mass: 100 mg, irradiation time: 45 min, 300 W Xe light. [b] Blank experiment, irradiation in the absence of any catalysts or illumination of the catalysts in Ar under above conditions. [c] Control experiment, irradiation of Ni-525 in pure H_2 under the above-mentioned conditions, indicating that no hydrocarbon was formed when there was no CO in the reaction mixture. [d] Commercial methanation Ni catalysts from Huaneng Ltd. [e,f] Irradiation with a solar simulator equipped with a cut-off filter ($\lambda > 400$ nm) for [e] 3 h and [f] 4 h.

genation is methane,[2] current catalyst can effectively catalyze the C–C bond formation under light irradiation, which has not been reported before. Importantly, there is no addition of a second metal or the use of active oxide support in the current study.

For Ni-550 and Ni-600, although the conversion of CO increased, the selectivity for the C_2–C_7 hydrocarbons decreased in return. The selectivity for the C_2–C_7 hydrocarbons followed the descending order of Ni-525 (60.1 %), Ni-500 (58.0 %), Ni-550 (37.5 %), and Ni-600 (25.8 %). In the first 15 minutes of light irradiation, the selectivity towards the C_2–C_7 hydrocarbons over Ni-525 can even reach 80 %, while long-time irradiation will lead to the hydrogenolysis of the hydrocarbons (Figure S7). Under irradiation, the temperature of the catalysis bed increased rapidly during the first 20 minutes, and stabilized at 150 °C after 40 minutes (Figure S8). The activation of CO requires a much higher temperature for a conventional Ni-based catalyst.[2,4,11,13] To check whether the current process is photoactivated or not, a control experiment was carried out at the same temperature without light irradiation. The result shows after 2 h of reaction at 150 °C, only less than 6 % CO was converted with the dominant product being CO_2 (Table S1).

Significantly, the Ni-525 catalyst is also active for higher hydrocarbon formation under visible-light irradiation ($\lambda > 400$ nm; Table 1, entry 10–11; the catalyst-bed temperature is around 81 °C). The conversion of CO reached 20.9 % while the selectivity of C_{2+} hydrocarbons was over 67.0 % in 3 h, suggesting that the NiO_x/Ni catalyst is effective even in visible light. Compared with UV/Vis light irradiation, the better selectivity towards C_{2+} was ascribed to the lower hydrogenolysis rate of hydrocarbons in visible light (Figure S7D). The above results indicate that the CO hydrogenation on Ni-525 is likely photoactived rather than a photothermal process. This photoactivation mechanism for Ni-containing photocatalysts was also reported by Gracia and co-workers in the photocatalytic transformation of CO_2 to methane.[10a]

The catalyst was quite stable and showed no obvious decrease in activity and selectivity after five catalytic cycles but a well-retained structure of the catalyst (Figures S9 and S10). Based on the above results, it is clear that under light irradiation, higher hydrocarbons can be produced over the NiO_x/Ni catalysts, and there is an optimized reduction temperature of the catalysts for chain propagation, that is, 525 °C. We speculated that, 1) the presence of metallic Ni is indispensable for the photocatalytic activity of CO hydrogenation; and that 2) the co-existence of Ni and NiO_x phases as a heterojunction photocatalyst may facilitate the photocatalytic C–C coupling reaction.[13e]

X-ray absorption near-edge structure (XANES) spectroscopy was employed to study the local coordination environment as well as the oxidation state of the catalysts during the reduction process (Figure 1 C–E). Figure 1 C shows that there is a monotonic decrease in the intensity of the Ni *K*-edge features of the catalysts with increasing reduction temperature, suggesting an obvious structural transformation, while the edge features for metallic Ni clearly appeared at 525 °C, indicating the co-existence of Ni and NiO_x on Ni-525. In case of Ni-600, the oxidation state is very close to that of metallic Ni. This conclusion was further confirmed by the extended X-ray absorption fine structure (EXAFS) results (Figure 1 D, Table S2). With increasing reduction temperature from 400 to 525 °C, the intensity of the Ni-Ni distance (metallic Ni) at 2.0 Å gradually appeared/increased while the scattering of the Ni-O and Ni-Ni (NiO) distances at 1.5 and 2.5 Å decreased, respectively.

In order to understand the distribution of NiO_x and Ni on the surface, in situ X-ray photoelectron spectroscopy (XPS) was used to track the surface state of the Ni-based catalysts. In the Ni 2p XPS spectra shown in Figure 1 E, the dominant peaks of NiAl-MMO and of those samples with a reduction temperature lower than 475 °C were attributed to oxides (both Ni^{2+} and Ni^{3+}), suggesting that those catalysts were only covered with oxides on the surface. This explains why those catalysts show almost no CO hydrogenation activity as normally the activation of the C–O bond requires metallic sites.[14] However, upon treatment in H_2 above 500 °C, the feature of Ni^0 $2p_{3/2}$ at 853.0 eV appeared at the expense of the oxidized Ni peaks. This observation indicates that the surface of Ni-500 to Ni-575 were a mixture of Ni oxides and metallic Ni. It is a generally accepted concept that the higher the reduction temperature, the lower the concentration of the oxide. When the reduction temperature reached 600 °C, the surface of the catalyst was dominated by metallic Ni. For catalysts reduced at this temperature, only a small amount of C_{2+} hydrocarbons were produced in the photocatalytic CO hydrogenation reaction. Based on the above results, we propose that the modulation of the Ni catalyst nanostructure by surface oxides changes its electronic structure and makes it capable of catalyzing the C–C coupling reaction, leading to the formation of higher hydrocarbons.

The surface geometry of the NiO_x/Ni catalysts was further revealed by TEM. For Ni-525, the nanoparticles are composed of face-centered cubic Ni particles (around 20 nm)

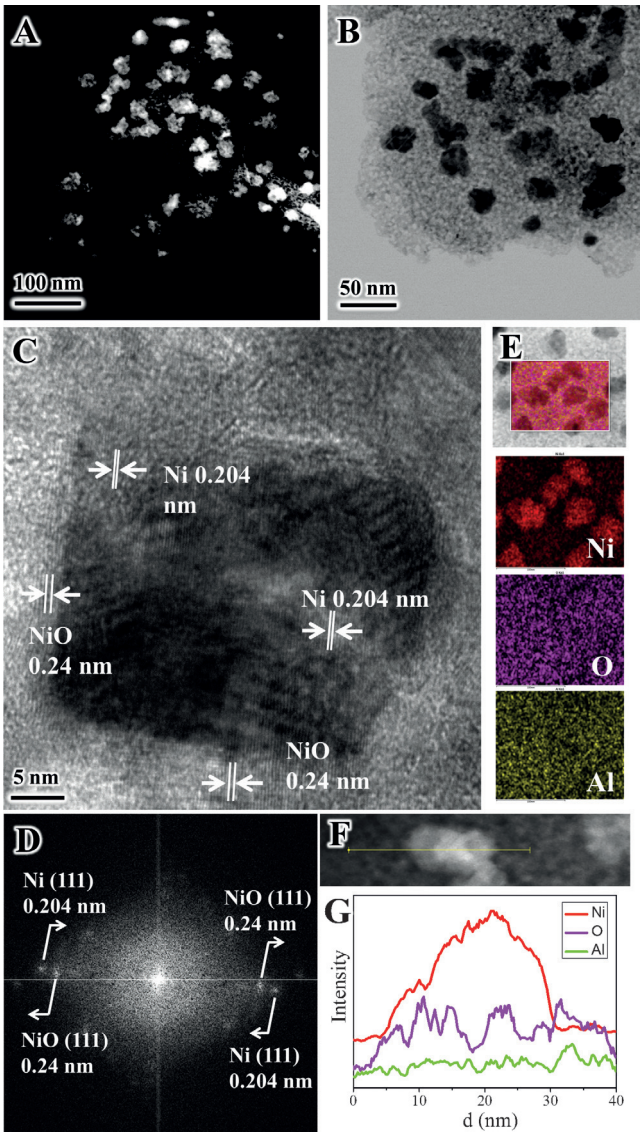

Figure 2. A) High-angle annular dark-field scanning TEM (HAADF-STEM) image. B) Annular bright-field (ABF) STEM image. C) High-resolution TEM (HRTEM) image and D) the corresponding FFT image, and E) the element mapping of the Ni-525. F) STEM image of one particle and G) the corresponding element (Ni, O, Al) intensity line-scan profiles.

partially decorated with a NiO_x overlayer (Figure 2 A–E). The coexistence of the two phases was further confirmed by a fast Fourier transform (FFT) pattern. Furthermore, the energy-dispersive spectra on selected spots of the Ni-525 nanoparticle (Figure S14) show dramatic variations of the Ni/O ratio, strongly suggesting the discrete nature of NiO_x layers on the surface of the Ni nanoparticles, which were also confirmed by a line scan over a single particle (Figure 2 F,G). For Ni-600, the particles were dominated with a metallic Ni phase and nearly no NiO_x was observed (Figure S15). From the above results, it is clear that the structure of Ni-x ($475 < x < 600$) is a Ni nanoparticle partially decorated by discrete NiO_x overlayers (Figure S12 C).

To investigate the reaction mechanism, first principle calculations have been carried out as well. Based on the experimental characterization results, two catalyst models of Ni(111) and 4O/Ni(111) (Figures S16 and S17) were constructed to represent the pure metallic Ni (Ni-600) and NiO_x/Ni (Ni-525) catalysts, respectively. For initial syngas (CO/H_2) conversion on Ni(111) and 4O/Ni(111) surfaces, only the most possible paths were shown in Figure 3. First, the calculation barriers of CO direct dissociation ($CO^* + * \rightarrow C^* + O^*$) on the above-mentioned two surfaces are 3.74 and 3.80 eV, respectively. For comparison, the H-assisted CO activation ($CO^* + H^* \rightarrow HCO^* + *$) has lower barriers of 1.37 and 1.30 eV, respectively, suggesting a dominant CO conversion to HCO species through hydrogenation on Ni and NiO_x/Ni surfaces (Figures S18 and S19).

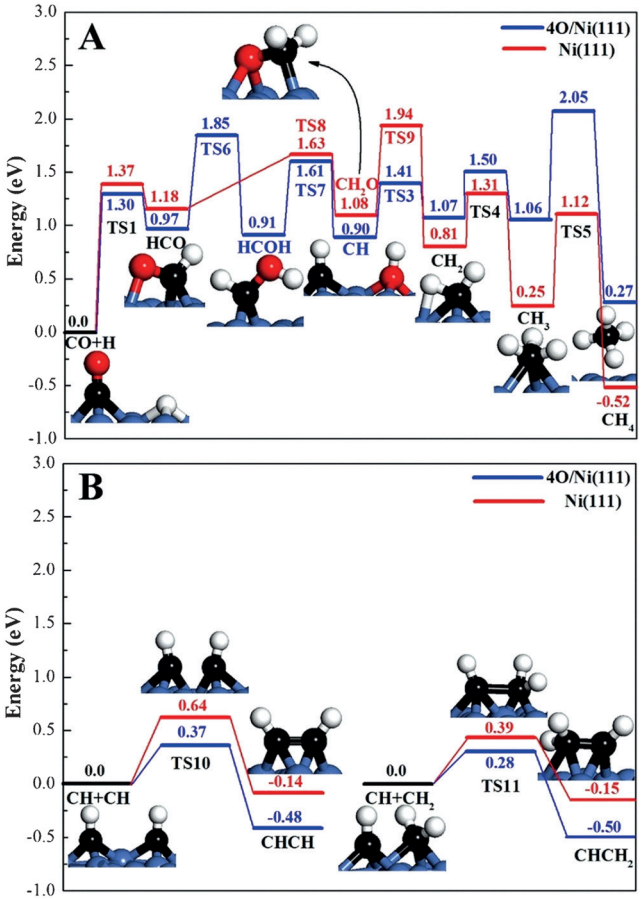

Figure 3. The potential-energy profile of the most possible reaction paths for syngas conversion on Ni(111) and 4O/Ni(111). A) CH_4 formation. B) C–C coupling.

In the following systematic study for possible reactions from HCO to CH_4 (Figure 3 A), the calculation results show that all steps on the Ni surface are exothermic, and its highest barrier is only 0.88 eV ($HCO^* + H^* \rightarrow CH_2O^* + *$), indicating that methane is the most favorable product on Ni both kinetically and thermodynamically. However, on a NiO_x/Ni surface, the CH hydrogenation to CH_2 is an endothermic process, and the CH_3 hydrogenation to CH_4 needs to over-

come a higher barrier of 0.99 eV, suggesting that the surface-dominant species may be CH_2 and CH_3 while CH_4 will not be the main product.

Finally, we further investigated the C–C coupling reactions on both surfaces (Figure 3B) and found that the barriers on a pure Ni surface are obviously higher than that on a NiO_x/Ni surface (0.64 vs. 0.37 eV and 0.39 vs. 0.28 eV). Therefore, it is inferred that the production of hydrocarbons was favored on the NiO_x/Ni surface (Figures S18 and S19), which agrees well with the experimental results. Under light irradiation, CO molecules are easily adsorbed on metallic Ni. Meanwhile, the existence of Ni^{3+} improves the efficiency for the carrier transformation (see Table S2).[9d,15] Indeed, the presence of photoactive holes and electrons of Ni-525 were also observed by electron spin resonance spectroscopy (Figure S20), which explains the relatively mild reaction conditions needed for the current FTS process.

In summary, novel Ni-based catalysts were synthesized by reducing the calcinated NiAl-LDH nanosheets, which exhibited an unexpectedly high selectivity for C_{2+} hydrocarbons in the CO hydrogenation reaction under visible-light irradiation. In situ XRD, XPS, EXAFS and TEM experiments show that the formation of hydrocarbons requires catalysts with the unique structure of Ni nanoparticles partially decorated with Ni oxide overlayers. Density functional theory calculations demonstrate that it is the modification of metallic Ni by surface oxides that changes the reaction path of the surface CH_x species, making the novel Ni-based catalyst excellent for C–C coupling in the CO hydrogenation reaction. This work demonstrates new opportunities for photocatalytic synthesis of high-value chemicals and fuels by using novel Ni-based nanostructured materials.

Acknowledgements

The authors are grateful for the financial support from the Ministry of Science and Technology of China (grant numbers 2014CB239402, 2013CB933100, and 2013CB834505), the Key Research Programme of the Chinese Academy of Sciences (grant number KGZD-EW-T05), the National Natural Science Foundation of China (grant numbers 1401206, 21473003, 21473229, 51322213, 21301183, 51172245, 91127005, 21401207, and 91545121) and the innovation foundation of the Institute of Coal Chemistry, Chinese Academy of Sciences. The computational resources for the project were supplied by the Tianhe-2 in Lvliang, Shanxi and the National Supercomputing Center in Shenzhen. The XAFS experiments were conducted in Beijing Synchrotron Radiation Facility (BSRF).

Keywords: Fischer–Tropsch synthesis · layered double hydroxides · nickel · photocatalysis · ultrathin nanosheets

How to cite: *Angew. Chem. Int. Ed.* **2016**, *55*, 4215–4219
Angew. Chem. **2016**, *128*, 4287–4291

[1] a) A. Y. Khodakov, W. Chu, P. Fongarland, *Chem. Rev.* **2007**, *107*, 1692; b) H. Jahangiri, J. Bennett, P. Mahjoubi, K. Wilson, S. Gu, *Catal. Sci. Technol.* **2014**, *4*, 2210; c) P. Zhai, G. Sun, Q. Zhu, D. Ma, *Nanotechnol. Rev.* **2013**, *2*, 547; d) H. Wang, W. Zhou, J. Liu, R. Si, G. Sun, M. Zhong, H. Su, H. Zhao, J. Rodriguez, S. Pennycook, J. Idrobo, W. Li, Y. Kou, D. Ma, *J. Am. Chem. Soc.* **2013**, *135*, 4149.
[2] B. C. Enger, A. Holmen, *Catal. Rev. Sci. Eng.* **2012**, *54*, 437.
[3] a) E. de Smit, B. M. Weckhuysen, *Chem. Soc. Rev.* **2008**, *37*, 2758;b) C. Yang, H. Zhao, Y. Hou, D. Ma, *J. Am. Chem. Soc.* **2012**, *134*, 15814.
[4] a) M. A. Vannice, R. L. Garten, *J. Catal.* **1979**, *56*, 236; b) S.-W. Ho, C.-Y. Chu, S.-G. Chen, *J. Catal.* **1998**, *178*, 34.
[5] S. He, C. Li, H. Chen, D. Su, B. Zhang, X. Cao, B. Wang, M. Wei, D. G. Evans, X. Duan, *Chem. Mater.* **2013**, *25*, 1040.
[6] J. van de Loosdrecht, A. J. van Dillen, A. A. van der Horst, A. M. van der Kraan, J. W. Geus, *Top. Catal.* **1995**, *2*, 29.
[7] C. Mirodatos, E. Brum Pereira, A. Gomez Cobo, J. A. Dalmon, G. A. Martin, *Top. Catal.* **1995**, *2*, 183.
[8] J. van de Loosdrecht, A. M. van der Kraan, A. J. van Dillen, J. W. Geus, *J. Catal.* **1997**, *170*, 217.
[9] a) X. Chen, S. S. Mao, *Chem. Rev.* **2007**, *107*, 2891; b) A. Kudo, Y. Miseki, *Chem. Soc. Rev.* **2009**, *38*, 253; c) F. E. Osterloh, *Chem. Soc. Rev.* **2013**, *42*, 2294; d) Y. F. Zhao, X. Jia, G. I. N. Waterhouse, L. Z. Wu, C. H. Tung, D. O'Hare, T. R. Zhang, *Adv. Energy Mater.* **2015**, 201501974; e) X. Guo, Z. Jiao, G. Jin, X. Guo, *ACS Catal.* **2015**, *5*, 3836.
[10] a) F. Sastre, A. V. Puga, L. Liu, A. Corma, H. Garcia, *J. Am. Chem. Soc.* **2014**, *136*, 6798; b) F. Sastre, A. Corma, H. Garcia, *Angew. Chem. Int. Ed.* **2013**, *52*, 12983; *Angew. Chem.* **2013**, *125*, 13221.
[11] X. Meng, T. Wang, L. Liu, S. Ouyang, P. Li, H. Hu, T. Kako, H. Iwai, A. Tanaka, J. Ye, *Angew. Chem. Int. Ed.* **2014**, *53*, 11478; *Angew. Chem.* **2014**, *126*, 11662.
[12] G. Fan, F. Li, D. G. Evans, X. Duan, *Chem. Soc. Rev.* **2014**, *43*, 7040.
[13] a) R. Burch, A. R. Flambard, *J. Catal.* **1982**, *78*, 389; b) P. Marginean, A. Olariu, *Appl. Catal. A.* **1997**, *165*, 241; c) S. Das, S. Thakur, A. Bag, M. S. Gupta, P. Mondal, A. Bordoloi, *J. Catal.* **2015**, *330*, 46; d) M. A. Vannice, R. L. Garten, *J. Catal.* **1980**, *66*, 242; e) S. J. A. Moniz, S. A. Shevlin, D. J. Martin, Z.-X. Guo, J. Tang, *Energy Environ. Sci.* **2015**, *8*, 731.
[14] J. Gao, C. Jia, J. Li, M. Zhang, F. Gu, G. Xu, Z. Zhong, F. Su, *J. Energy Chem.* **2013**, *22*, 919.
[15] Y. F. Zhao, Q. Wang, T. Bian, H. J. Yu, H. Fan, C. Zhou, L. Z. Wu, C. H. Tung, D. O'Hare, T. R. Zhang, *Nanoscale* **2015**, *7*, 7168.

Received: December 7, 2015
Revised: February 1, 2016
Published online: February 24, 2016

